Effect of the Specimen Dimensions and the Test Speed on the Fracture Toughness of iPP by the Essential Work of Fracture (EWF) Method

MARIA LLUÏSA MASPOCH[1], DIDAC FERRER[1], ANTONIO GORDILLO[2], ORLANDO O. SANTANA[2], ANTONIO B. MARTINEZ[1]

[1] Departament de Ciència dels Materials i Enginyeria Metal·lúrgica, Universitat Politècnica de Catalunya, Av. Diagonal 647, 08028-Barcelona, Spain

[2] Centre Català del Plàstic, C/Colom 114, 08222-Terrassa, Spain

Received 27 July 1998; accepted 22 October 1998

ABSTRACT: The fracture parameters of an isotactic polypropylene are studied by the essential work of fracture method. The influence of the specimen height, width and thickness and the effect of the test speed are investigated. Results show that this method is very useful for studying the plane-stress fracture of this kind of materials in form of films and sheets. Varying the width (30 to 60 mm) and the test speed (2 to 100 mm/min) has no relevant influence, whereas the results are only length independent in a range from 40 to 100 mm. The influence of the thickness is very high, obtaining an important decrease of the specific essential work as the thickness is increased in a range from 38 to 2500 μm. This result is justified with the fracture surfaces obtained, observed by SEM, in which an evolution of the fracture behavior is seen as a function of thickness (38, 100, 500, 1000, 2500 μm). © 1999 John Wiley & Sons, Inc. J Appl Polym Sci 73: 177–187, 1999

Key words: work of fracture; toughness; polypropylene; deeply double-edge notched tensile; fracture of films and sheets

INTRODUCTION

An experimental method, called the Essential Work of Fracture (EWF) and developed by Mai and Cotterell[1,2] following the Broberg's theoretical idea,[3] is being increasingly used for the toughness determination on polymeric films and sheets. According to the theory, the value that represents the toughness, namely the specific essential work of fracture (w_e), is a material parameter, independent on the specimen geometry. However, some aspects of this theory remain controversial, and much investigation is being done to assess the dependence of the fracture parameters on different variables and verify if w_e represents an intrinsic material property.[4–15] In this study, the variables studied are the specimen thickness (t), the width (W) and the length (Z) of Deeply Double Edge Notched Tension (DDENT) specimens (Figure 1) and the crosshead speed (v).

The main effort of this study is done on the thickness dependence of the fracture parameters of an isotactic polypropylene (iPP), since this method allows to determine the material's toughness in a wide thickness range in which the stress modes prevailing can evolve from a plane-stress state for thinner films to a mixed-mode (between plane-stress and plane-strain states) as the thickness is increased. According to the Linear Elastic Fracture Mechanics (LEFM), the toughness (K_{IC})

Correspondence to: M. L. Maspoch.

Journal of Applied Polymer Science, Vol. 73, 177–187 (1999)
 CCC 0021-8995/99/020177-11

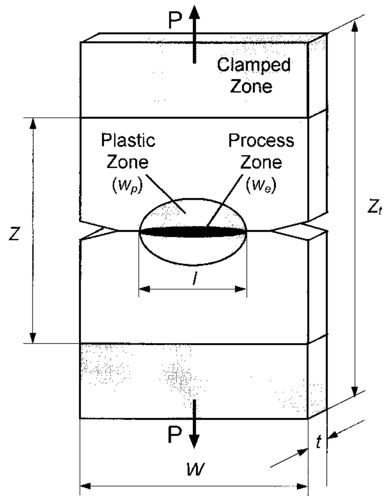

Figure 1 DDENT specimen, showing the dimensions and the plastic and process zones.

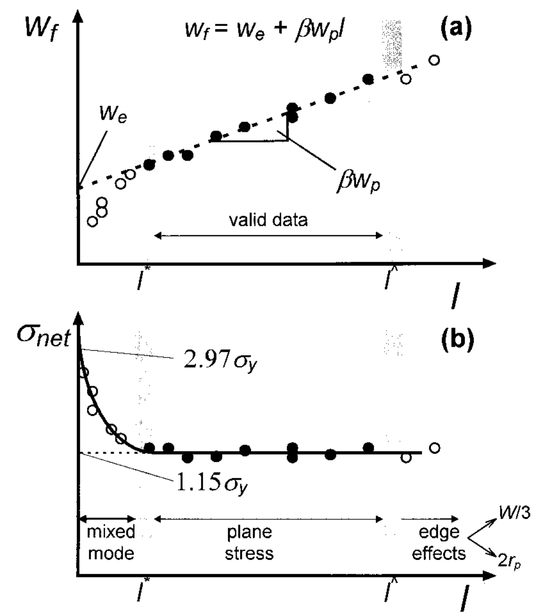

Figure 3 (a) Schematic representation of the specific total work of fracture against the ligament length to determine the specific essential work of fracture (w_e). (b) Plot of the net stress against the ligament length to identify the stress–strain states in function of l.

depends on t as shown in Figure 2.[16] It has a maximum for $t = B_0$ which is considered as the plane-stress fracture toughness value. As t increases, a mixed-mode is found and the toughness decreases until $t = B_C$, at which the plane-strain conditions prevail and K_{IC} becomes constant. The extrapolation of this considerations, which are well established for the LEFM, to the Post Yield Fracture Mechanics (PYFM) by the EWF method is discussed in this work.

THEORY

Following Broberg's idea, a test procedure for measuring the plane-stress essential work of fracture was developed. According to the theory, the total work done to break a notched specimen (W_f) is the sum of two terms, called the Essential and Non-Essential Work of Fracture (W_e and W_p respectively). The former is related to the instability of the crack tip (where the real fracture process occurs) and it is the energy dissipated in the process zone (Figure 1), being proportional to the ligament section (lt). The latter is associated with the plastic work done in a volume around the process zone, called the plastic zone, and it is proportional to this volume ($\beta l^2 t$):

$$W_f = W_e + W_p = w_e l t + w_p \beta l^2 t \tag{1}$$

$$w_f = W_f / lt = w_e + \beta w_p l \tag{2}$$

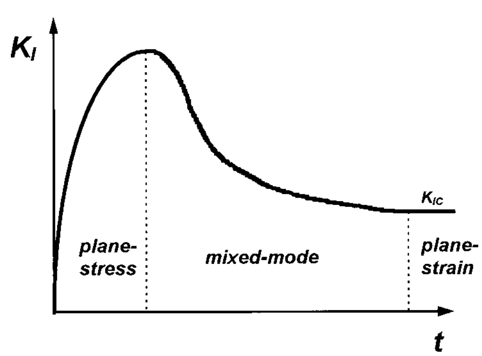

Figure 2 Evolution of the toughness in function of the thickness varying with the stress–strain state, according to the LEFM.

According to the equation 2, if the specific work of fracture (w_f) is plotted against the ligament length (l), a linear relation is obtained, which Y-axis intercept and slope are w_e and βw_p respectively. Thus, it is obvious that the EWF procedure is a simple method that consists of testing different ligament length specimens, registering W_f for each, plotting the $w_f - l$ diagram and calculating the best fit regression line which gives w_e and βw_p, as represented in Figure 3a. Either DDENT or SENT specimens can be used indistinctly.

Following the ESIS protocol of EWF,[17] two restrictions must be satisfied for the validity of the theory. Firstly, the minimum ligament length must ensure that the specimen is tested under plane stress conditions (it is usually considered that this occurs when $l > (3 - 5)t$). However, the verification of the ligament length (l^*) for which the transition of plane stress to mixed mode conditions occurs may be verified by plotting the maximum net stress, σ_{net} (maximum load divided by the original section), obtained during the DDENT specimens tests against their initial ligament length. Following the Hill's predictions,[18] a DDENT specimen in pure plane stress solicitation has a σ_{net} value which is 1.15 times the yield stress (σ_y), which raises to $2.97\sigma_y$ in pure plane strain conditions (Figure 3b). Secondly, the maximum l value must keep the specimen out from edge effects, and must also ensure that the ligament is fully yielded before the crack propagation. For these purposes, the ligament length must satisfy:

$$l^* < l < \hat{l} = \min(W/3,\ 2r_p) \qquad (3)$$

where W is the specimen's width and $2r_p$ is the plastic zone size generated by the crack tip, calculated with the following equation (5) for a line plastic zone:

$$2r_p = (\pi/8)(Ew_e/\sigma_y^2) \qquad (4)$$

where E and σ_y are respectively the Young's modulus and the yield stress of the material obtained in comparable test conditions.

EXPERIMENTAL

Material

The material studied was an homopolymer iPP film grade (Escorene 4563F1) from Exxon, received as non-oriented films of 38 and 100 μm thick (obtained by cast extrusion), and in form of pellets, which were transformed by compression molding into 0.5, 1 and 2.5 mm thick sheets. This transformation was realized as it follows: the material was put into a steel frame with a thickness of 0.5, 1 or 2.5 mm between two steel plates. After heating and melting the material in the press during 1 min at 185°C, the pressure was gradually increased with stages at 20, 50, 80 and 100 bar of 1 min long, with air expulsion between each stage. Immediately after, the mold was introduced between room temperature water-tempered plates at 100 bar for 3 minutes. With the aim of studying the morphological difference between cast and compression molded specimens, wide-angle X-ray scattering patterns were obtained with a Statton-type chamber. It could be observed from this study that cast and compression specimens had the same crystalline structure, but not the same crystallinity, since the cast film specimen exhibited a considerably lower intensity of the patterns than the compression molded specimen.

Tensile Tests

At least 5 specimens were tested (for each set) on an universal testing machine at different crosshead speeds of 2, 20 and 100 mm/min at room temperature. The specimens were cut from the films and sheets with a normalized die (excepting 2.5 mm specimens which were too stiff) obtaining ASTM-D638 standard dumbbell specimens (Type IV). The stress and strain values at maximum load (σ_y, ϵ_y) as well as the Young's modulus (E) were evaluated.

Fracture Tests

DDENT specimens (Figure 1) were prepared by cutting the films and sheets into rectangular coupons of $Z = W = 60$ mm ($Z_t = 100$ mm). Since the influence of the geometric parameters W and Z was studied, specimens with $W = 30$, 45, 60 mm ($Z = 60$ mm) and $Z = 20$, 40, 50, 60, 80, 100, 120, 150 mm ($W = 60$ mm) were also prepared with the 100 μm films. Initial notches were made perpendicularly to the traction direction with a fresh razor blade mounted on a laboratory attachment designed for this purpose, obtaining for each set at least 20 specimens with ligament lengths varying between 1 and 20 mm with the distribution recommended by the ESIS protocol.[17] For the 38 and 100 μm films, the ligament lengths were measured before the test from both sides using a traveling microscope, whereas for the sheets they were measured after the test (perpendicularly to the notches plane) for more accuracy on the measure. The thickness of each specimen was measured in the center of the ligament before the tests, using a magnetic-inductive coating thickness measurer (Neurtek, Spain) with a precision of 1 μm. The influence of the test rate was also investigated on 100 μm thick spec-

Table I Scheme of the Tests Realized for the Study of the Influence of the Thickness (*t*), the Gage Length (*Z*), the Width (*W*), and the Test Speed (*v*) on the EWF Parameters

Prep. Method	t (μm)	Z (mm)	W (mm)	v (mm/min)
cast	38	60	60	2
cast	100	60	60	2
cast	100	60	60	20
cast	100	60	60	100
cast	100	20	60	20
cast	100	40	60	20
cast	100	50	60	20
cast	100	60	60	20
cast	100	80	60	20
cast	100	100	60	20
cast	100	120	60	20
cast	100	150	60	20
cast	100	60	30	20
cast	100	60	45	20
cast	100	60	60	20
compr. mold.	500	60	60	2
compr. mold.	1000	60	60	2
compr. mold.	2500	60	60	2

imens ($W = Z = 60$ mm) at $v = 2$, 20 and 100 mm/min, whereas the thickness dependence was evaluated on the 38, 100, 500, 1000 and 2500 μm thick specimens at 2 mm/min, all them at room temperature. The tests realized are summarized in Table I.

RESULTS AND DISCUSSION

Tensile Properties

The iPP studied showed a typical viscoelastic dependence of E and σ_y on v, as can be seen in Table II. The mechanical properties are also highly influenced by the thickness. In fact, it seems that the preparation method is more important than the variation in t, since changing from 38 to 100 μm has little effect on both E and σ_y in comparison with changing from 100 μm (cast) to 500 μm (compression). Relating this with the results of the X-Ray scattering, one can therefore attribute the high differences observed on the mechanical properties to the variation in cristallinity of both films and sheets specimens. One can therefore expect that fracture results can be influenced by this change in cristallinity.

Table II Influence of the Thickness, the Preparation Method, and the Test Rate on the Mechanical Properties

t (μm)	Prep. Method	v (mm/min)	E (MPa)	σ_y (MPa)
100	cast	2	616	19.98
100	cast	20	689	23.92
100	cast	100	700	27.25
38	cast	2	611	17.91
100	cast	2	616	19.98
500	compr. mold.	2	949	27.05
1000	compr. mold.	2	939	27.83

Fracture Behavior

For films and thin sheets with $t \leq 1000$ μm the fracture of DDENT specimens was completely stable, obtaining load vs. displacement diagrams like those shown in Figure 4 (it should be noticed that the load is normalized by the ligament section to obtain comparable curves). On the other hand, the 2500 μm sheets showed an unstable fracture at the same speed (2 mm/min). As the fracture behavior of the thicker sheets was not stable, and this is a requirement to apply the theory, the EWF approach has not been applied to them. In Figure 5a, the curves obtained at 20 mm/min with specimens of 100 μm of different initial ligament lengths are showed. It can be observed that their shape is practically identical for the different initial ligament lengths, indicating that the fracture mode seems to be indepen-

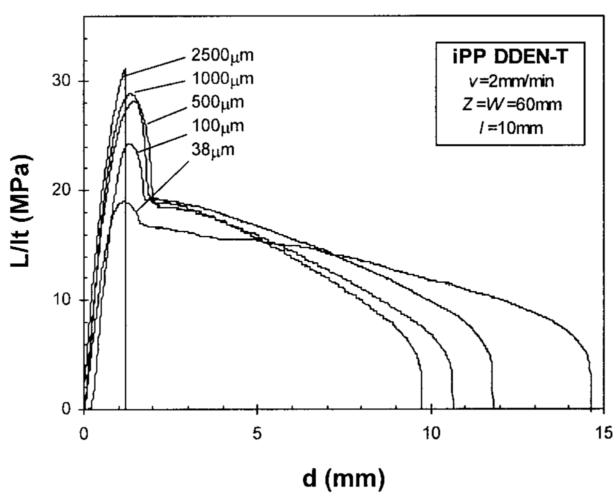

Figure 4 Normalized load vs. displacement curves obtained with DDENT specimens of different thickness, with a common ligament length of about 10 mm.

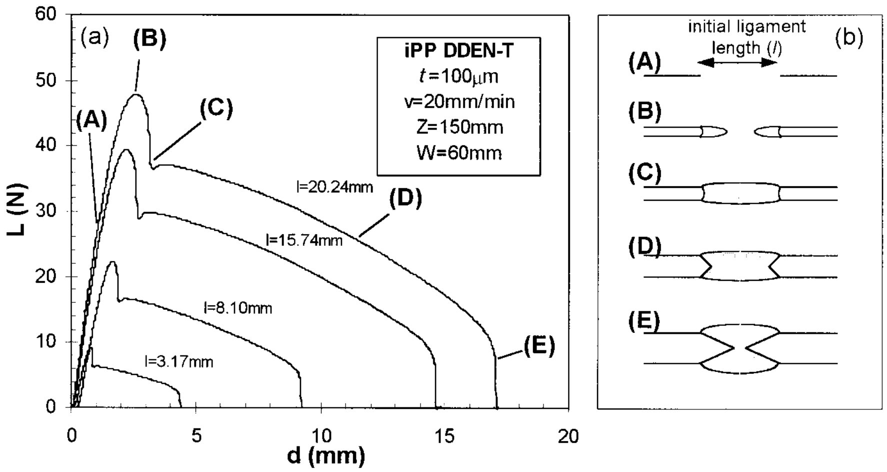

Figure 5 (a) Load vs. displacement curves of the DDENT specimens with various different ligament length. (b) Schematic representation of the ligament zone during the loading.

dent of ligament length. The ligament area was observed during the test using a microscope equipped with a camera (Figure 5b is a schematic representation of its evolution): there is at first a linear elastic behavior (**A**), followed by the generation of two line plastic zones that grow in each crack-tip as the load increases due to the high stresses concentrated there. After the maximum load (**B**), the plastic zones meet each other (the entire ligament is yielded) and subsequent necking starts on the crack tips, producing a marked load drop until the whole ligament is necked (**C**). This occurs very rapidly and, at this moment, the crack starts to grow across the necked zone (**D**) until fracture occurs (**E**).

However, not all the DDENT specimens had the same behavior, which was influenced by the thickness. From the ligament observation during the tests, it followed that the ligament was not fully necked when the crack started to grow on the thicker sheets ($t \geq 500$ μm) or, what is the same, that the propagation started between stages **B** and **C.**

While varying the width had no significant influence on the shape of the load-displacement curves, increasing the length 'shifted the curve to the right,' producing a clear decrease in the slope of the stage **A** and an increase in the final displacement, although it did not modify substantially neither the maximum load nor the total energy (Figure 6). This means that, initially, the longest specimens stored more elastic energy, which was restored later and used to propagate the crack. The effect of the test speed on the DDENT specimen behavior was in accordance with that observed on the tensile tests: as v was increased, the maximum load and the initial slope increased as well, whereas the final elongation was reduced (Figure 7).

As it has been explained before, the specific fracture work (w_f) was plotted against the ligament length for each set, and a linear relation was calculated with the plane-stress data. From the maximum load of the load-displacement curves, the value of σ_{net} was calculated for each specimen in order to verify the Hill's prediction.[18] For this purpose, the σ_{net} vs. l diagram was plotted, and the data position was compared with the

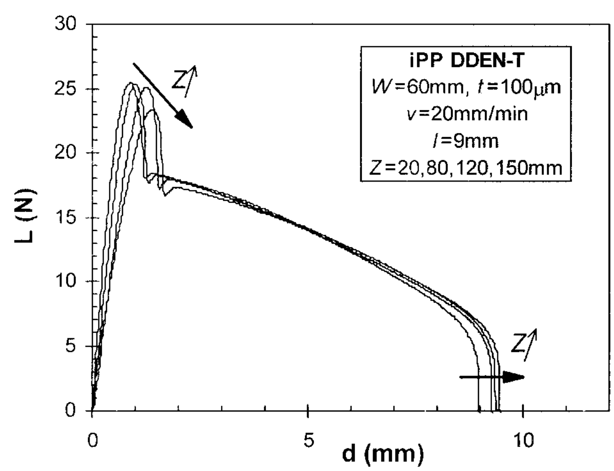

Figure 6 Evolution of the load vs. displacement curves of the DDENT specimens when the specimen length is varied from 20 to 150 mm.

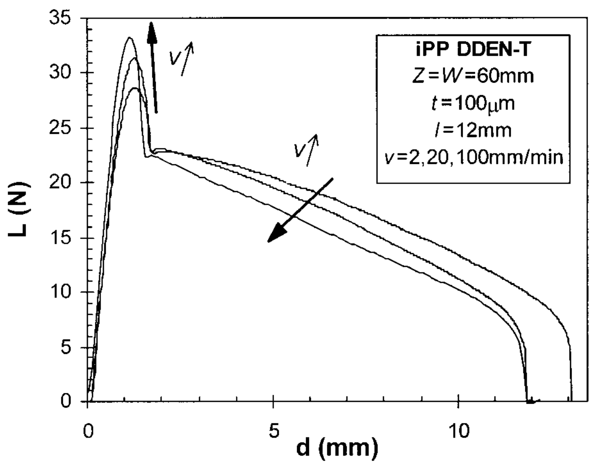

Figure 7 Evolution of the load vs. displacement curves of the DDENT specimens varying the test rate from 2 to 100 mm/min.

$1.15\sigma_y$ value. In each case, the σ_y used for calculation was the maximum stress at the same test rate and with the same thickness as that of the DDENT specimens tests. Moreover, the $w_f - l$ data were also fitted with a power law relation of the form:

$$w_f = Al^n \tag{5}$$

The advantage of this fitting is that this kind of equation seems to correlate very well all the data (mixed-mode and plane-stress with a single function), although it has no theoretical justification. For its resemblance to the J-integral approach, it has been calculated for different materials by different authors.[4,6,11,12] Used as a "supplementary fitting," we think that it can help to elucidate if a w_e and βw_p have a dependence on a variable or not: if there is not any important change in the A and n values calculated, it can be concluded that the fracture parameters are independent of the variable in the range studied.

Effect of test speed on the EWF fracture parameters

As explained before, the test rate influence was investigated on 100 μm films with W and Z of 60 mm. The Figure 8a shows the w_f vs. l plots of specimens tested at 2, 20 and 100 mm/min. Filled symbols correspond to specimens tested under plane stress conditions, while open symbols refer to values obtained under a mixed-mode state. The distinction between the points obtained under each stress state has been done following the Hill's analysis. Plotting σ_{net} vs. l (Figure 8b) it can be seen that the stress state transition occurs for a ligament length value of $l^* \approx 5$–6 mm. The regression lines of the plane stress data give us the w_e and βw_p values, which are listed in Table III. From the results, it seems that both w_e and βw_p values decrease as the test rate is increased, indicating that the material is slightly tougher at lower speeds. Even though this result can be justified by the viscoelastic nature of polymers, the difference is so low that probably the change in the test speed from 2 to 100 mm/min does not actually influence, and what seems a decrease in the EWF parameters may only be due to the experimental error. A little decrease is observed in the A value, but any logical tendency in the value of n cannot be observed, what can corroborate the experimental error supposition.

Effect of specimen width on the EWF fracture parameters

The aim of studying the influence of W was to verify the restriction of equation 3 for the maxi-

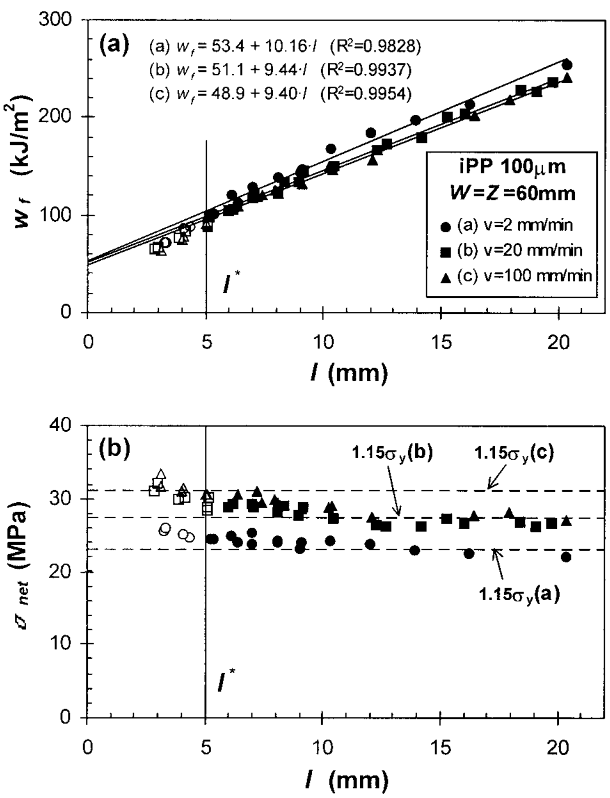

Figure 8 Specific total work of fracture vs. ligament length (a) and maximum net stress vs. ligament length (b) plots for DDENT specimens tested at different speeds.

Table III EWF Parameters in Function of the Test Speed

ν (mm/min)	w_e (kJ/m^2)	βw_p (MJ/m^3)	A (kJ/m^2)	n	$2r_p$
2	53.4 ± 3.9	10.16 ± 0.37	32.15	0.6914	32.4
20	51.1 ± 2.4	9.44 ± 0.19	31.61	0.6699	24.2
100	48.9 ± 2.4	9.40 ± 0.20	28.98	0.6978	18.1

mum ligament length, $l^\wedge$. The plot (Figure 9a) gives the values listed in Table IV, show that the fracture behavior does not seem to be influenced by the different value of W (and thus $l^\wedge$) for each set. For example, for $W = 30$ mm it is impossible to observe any transition at $l = W/3 = 10$ mm, neither in Figure 9a nor 9b. This agrees with the Hashemi's observations on polycarbonate films.[5] In fact, we think that the criterion of $W/3$ is too restrictive, at least for this material. After equation 4, the other limit for the maximum length, $2r_p$, has also been calculated, and it gives higher values than 20 mm for $W = 30$, 45 and 60 mm respectively, using E and σ_y values obtained at 20 mm/min with the 100 μm dumbbell specimens, which are more reasonable values than $W/3$.

According to the best fit regression lines calculated, w_e increases slightly with W, whereas βw_p has an opposite tendency. However, the values found are again quite similar and can be affected more by the experimental error than by the true influence of the width, and this seems to be confirmed by the A and n values obtained, which do not have a sensitive evolution in function of W.

Effect of specimen height on the EWF fracture parameters

The w_f vs. l data obtained with the different length specimens (with $t = 100$ μm, $W = 60$ mm and $v = 2$ mm/min) have been plotted (Figure 10a), in which is difficult to distinguish the influence of Z. On the other hand, in Figure 10b the σ_{net} vs. l data show slight different values as a function of Z, though a logical tendency cannot be found. As before, the best fit lines have been calculated with data corresponding to $l > 6$ mm, and the results obtained are listed in Table V and showed graphically in Figure 11. It can be seen that the specimens in the range from 40 to 100 mm long have similar w_e and βw_p values, while the shortest and longest specimen disrupt the tendency. This can be explained from the visual observation of the tests: the specimens with $Z > 100$ mm get highly undulated in their own plane during the tests, thus probably modifying the stress distribution in the ligament zone. On the other side, those with $Z = 20$ mm seem to be too far away from the "infinite plate" case, being the result probably influenced by the crosshead edges proximity to the fracture region. Thus, the calculation of an average of both essential and non-essential parameters in the aforementioned range (40–100 mm) gives $w_e = 49.16$ kJ/m^2 and $\beta w_p = 9.65$ MJ/m^3. The independence of the variation of the specific fracture work with ligament length from Z is also found in the A and n values for this range.

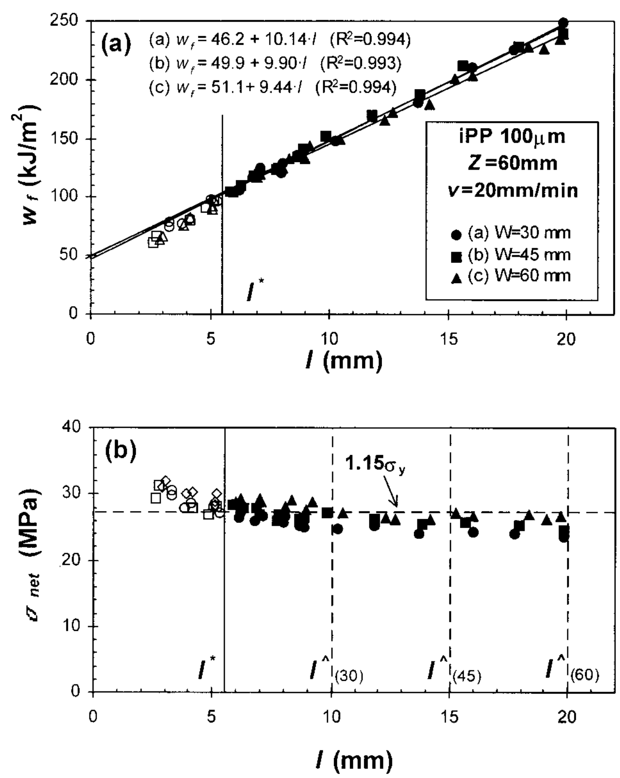

Figure 9 Specific total work of fracture vs. ligament length (a) and maximum net stress vs. ligament length (b) plots for different width DDENT specimens.

Table IV EWF Parameters in Function of the Specimen Width

W (mm)	w_e (kJ/m^2)	βw_p (MJ/m^3)	A (kJ/m^2)	n	$2r_p$
30	46.2 ± 2.6	10.14 ± 0.23	32.69	0.6629	21.8
45	49.9 ± 2.8	9.90 ± 0.24	31.84	0.6767	23.6
60	51.1 ± 2.4	9.44 ± 0.19	31.61	0.6699	24.2

Effect of thickness on the EWF fracture parameters

The w_f against l diagram for different thickness DDENT specimens is showed in Figure 12a. Again, the plot of σ_{net} vs. l (Figure 12b) is used to separate data obtained under each stress state. Three remarks can be extracted from these results.

Firstly, the plane stress points do not lay exactly on the value predicted by Hill. Thus, while the film data are very close to $1.15\sigma_y$, the 500 and 1000 μm sheets values do not fulfill so well the prediction, laying near σ_y as if double notches did not produce any constraint.

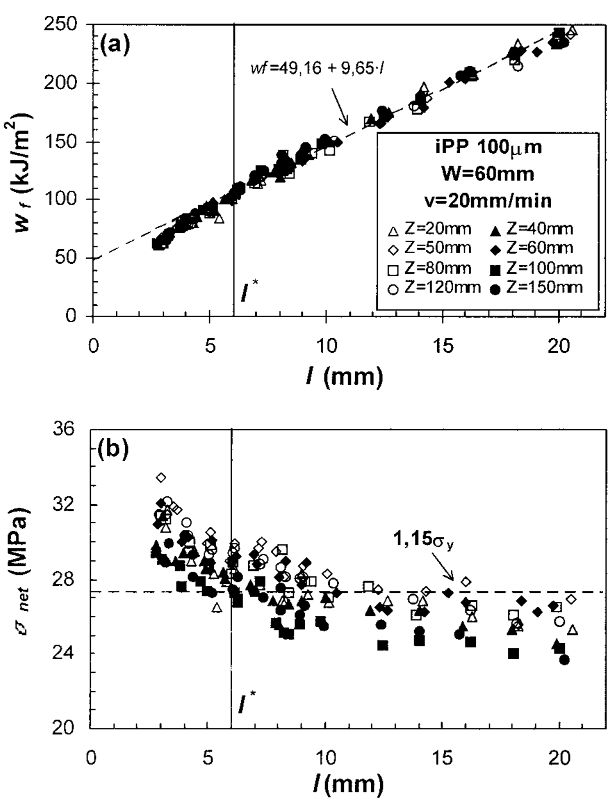

Figure 10 Specific total work of fracture vs. ligament length (a) and maximum net stress vs. ligament length (b) plots for different length DDENT specimens.

Secondly, there is not an exact l^* value at which the transition occurs, as the growth of the σ_{net} when l is reduced is not very marked. However, both Figures 12a and 12b allow us to situate a transition at $l^* \approx 5$ mm for films and $l^* \approx 6$ mm for sheets (in Fig. 12a, it can be observed that the mixed-mode data are found to be situated under the regression lines, what is helpful to situate l^*). Obviously, this value is rather far from the $l^* = (3 - 5)t$ suggested by the ESIS,[17] but other works[6,7,9] have already found similar l^* values. For the specimens of $t = 1000$ μm, it can be seen in Table VI that the value of $2r_p$ is rather below the other maximum ligament size criterion, $W/3$, and thus, according to equation 3, the points of longer ligament should not be considered for the regression line calculation. However, the σ_{net} vs. l plot shows that the values corresponding to $l > 12$ mm have the same stress level, and therefore a similar behavior, than those situated between $l^* < l < 12$ mm, despite that the ligament is not fully yielded when necking starts (moreover, the shape of the load-displacement curves does not change). Otherwise, it is important to

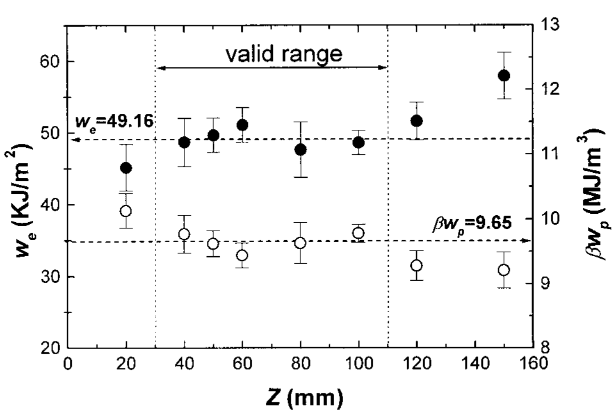

Figure 11 Specific essential work (full circles) and specific plastic work (open circles) vs. specimen length, obtained with specimens of $W = 60$ mm and $t = 100$ μm at $v = 20$ mm/min. The mean w_e and βw_p values of the valid range are indicated.

Table V EWF Parameters in Function of Specimen Height

Z (mm)	w_e (kJ/m^2)	βw_p (MJ/m^3)	A (kJ/m^2)	n	$2r_p$
20	45.15 ± 3.23	10.13 ± 0.27	29.21	0.7052	21.3
40	48.68 ± 3.36	9.77 ± 0.29	31.67	0.6736	23.0
50	49.69 ± 2.40	9.62 ± 0.20	31.72	0.6706	23.5
60	51.11 ± 2.43	9.44 ± 0.19	31.61	0.6690	24.2
80	47.66 ± 3.86	9.63 ± 0.32	29.84	0.6896	22.5
100	48.65 ± 1.68	9.78 ± 0.14	30.98	0.6821	23.0
120	51.62 ± 2.63	9.28 ± 0.23	29.95	0.6892	24.4
150	57.93 ± 3.28	9.21 ± 0.28	31.65	0.6806	27.4

consider that, as suggested by Hashemi,[5] equation 4 may not be very accurate (it may be highly dependent on the plastic zone shape, and also on the E value determination method).

Thirdly, the behavior of the specimens of $t = 2500$ μm must be analyzed particularly. As it is has been explained before, they showed a brittle behavior; after the maximum, the crack propagation was unstable. Obviously, this has repercussions on the w_f value, which is considerably lower than stable specimens, as can be seen on Figure 12a (($*$) correspond to unstable fracture, whereas ($\times$) correspond to stable fracture). It should also be noticed that only the two shortest ligament specimens showed a stable failure, obtaining values comparable to those of lower thickness sheets. The reason why there are so few values is that we have only considered the specimens whose crack propagated in the plane of the notches, having observed many irregular propagations in the other specimens.

With the plane stress data, the regression lines have been calculated (Table VI). A high dependence on thickness has been obtained, as the toughness of the 38 μm films is about three times the toughness of the 1000 μm sheets. Even though the dispersion in Figure 12a (and consequently the experimental error) is quite important, the tendency of a growth of w_e as t is reduced can be confirmed for this material in this thickness range. Such a dependence goes in the opposite direction that those of other similar investigations.[5,12,15] The influence of t on the plastic work item, βw_p, is less clear, and we can only say that for a same transformation method (cast or compression molding) it slightly decreases with an increase of the thickness, thus suggesting that the transformation method influence should be taken into account (since it is related to variations in cristallinity).

Thus, analyzing the effect of the thickness on the toughness parameter, w_e, it seems obvious that it would have been more logical to obtain an opposite tendency, since the values reported characterize plane-stress fracture and, according to Figure 2, this occurs in a range of thickness under B_o, in which, theoretically, an increase in the thickness produces a gain in toughness. As this

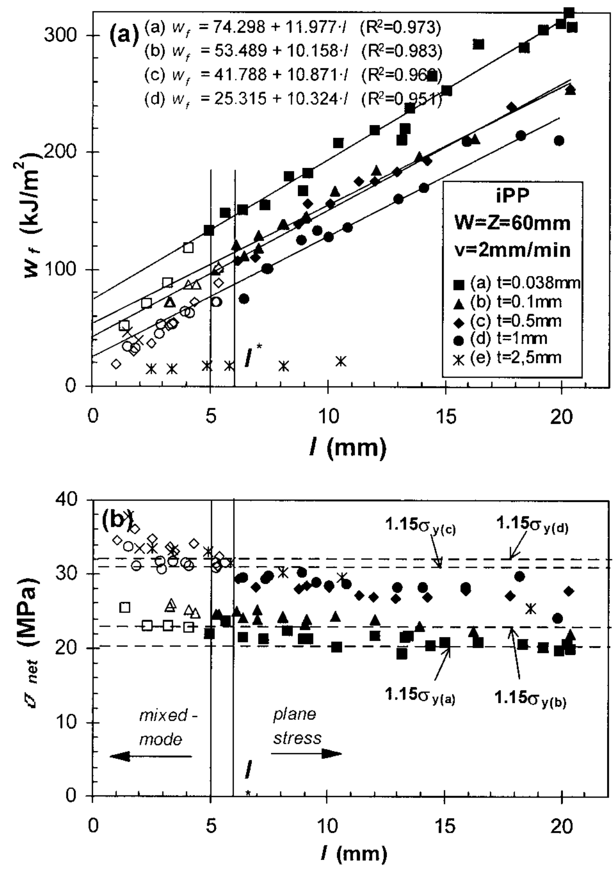

Figure 12 Specific total work of fracture vs. ligament (a) and maximum net stress vs. ligament length (b) plots for different thickness DDENT specimens.

Table VI EWF Parameters in Function of Thickness

t (μm)	w_e (kJ/m^2)	βw_p (MJ/m^3)	A (kJ/m^2)	n	$2r_p$
38	74.3 ± 6.5	11.98 ± 0.47	43.08	0.6598	55.6
100	53.5 ± 4.0	10.16 ± 0.37	32.16	0.6914	32.4
500	41.8 ± 8.5	10.87 ± 0.69	18.89	0.8967	21.3
1000	25.3 ± 9.3	10.32 ± 0.74	21.03	0.7874	12.0
2500	—	—	—	—	—

results were deserving of more investigation, a fractographic study by SEM was carried out. Fracture surfaces were observed in a JEOL JSM 6400 scanning electron microscope after gold coating. A broken specimen of each thickness was observed perpendicularly to the fracture plane, excepting the 38μm one, that was too thin to be subjected (Figure 13). For comparison purposes, these fractured specimens had the same initial ligament length (about 5 mm).

From a lateral visual observation, all specimens excepting the thickest one seemed to have undergone a similar ligament deformation, but from the observation of the fracture surface by SEM, it follows that there is an evolution of the fracture behavior when the thickness is increased. One can observe three types of fractured areas: the first one is a highly deformed by tearing region (that we called T-region), situated on the surfaces of the specimen, and that produces a necking. The second one is a wedge-shaped zone (WS-region), limited by the notch and the T-region, where it has also been plastic deformation but in a lower level than in the previous region. Both T and WS regions are formed in stable fracture processes. Finally, the third type is a pseudo-brittle fracture surface (PsB) that appears when the crack growth is unstable.

As can be seen in Figure 13, the relative proportion of T-region compared to WS-surface is reduced as the thickness increases: the ligament of the 100 μm specimen is almost totally deformed plastically by tearing, whereas in both 500 and 1000 μm specimens the two distinct stable fracture zones appear (T and WS). In the 2500 μm specimen, almost all the initial crack growth is done in a WS-region (a very small T-area can be observed at both sides), until a stable-unstable growth transition occurs, which was not observed in the other thickness specimens, that produces a PsB-region. From this observations, one could conclude that T and WS areas correspond approximately to plane-stress and plane-strain regions respectively, and even though theoretically plane-stress conditions are met for all specimens (according to Hill's analysis in Figure 12b), the plane-strain component plays a higher role as t increases, thus decreasing the specific essential fracture work. At a critical thickness value (2500 μm in this case), the brittle behavior appears. Such a behavior has already been observed by other investigators (19, and references there in), and is known as "ductile instability." It is nevertheless necessary to do more investigation, and a further study will deepen in this field.

CONCLUSIONS

It has been shown that the EWF method can be successfully applied to measure the fracture pa-

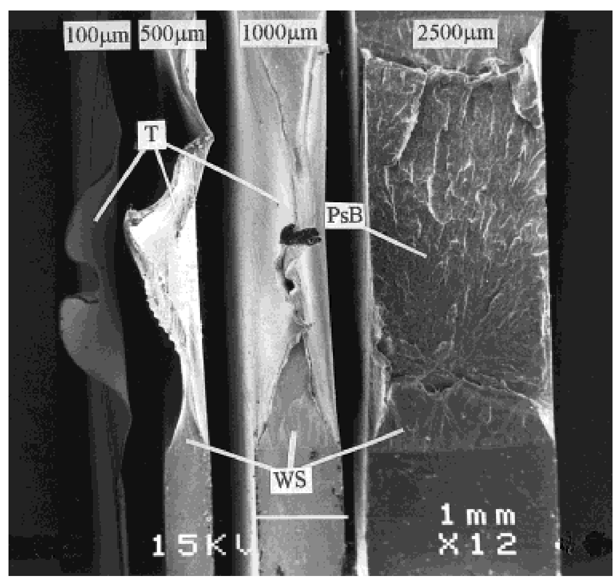

Figure 13 Scanning electron micrograph of fracture surfaces of different thickness DDENT specimens, indicating the distinct fracture zones: Tearing (T), Wedge-shaped (WS), and Pseudo Brittle (PsB) regions.

rameters of an iPP grade. The influence of different parameters has been studied, and from the results obtained one can say that the width and the test speed have no sensitive influence neither on the w_e nor the βw_p values in the ranges studied. Similar conclusions have been reported by Hashemi[6,7] and Chan and Williams.[8] Since one can expect to obtain an appreciable effect of the rate at impact rates, our group is working to apply the EWF method at high speed. No influence appears either varying the gage length in a range from 40 to 100 mm. Thus, values of 49 kJ/m^2 and 9.6 MJ/m^3 for the specific essential and non-essential works of fracture respectively can be accepted for the iPP studied with a thickness of 100 μm. As observed by other investigators,[6,7,9,15] the lower limit for the ligament length (l^*) seems not to be subjected to the $l^* = (3 - 5)t$ criterion, being rather above the predicted value. Moreover, a constant value of about 5–6 mm has been found, independent of the thickness in the range studied. Since it is not obvious to choice a low limit for plane stress data, and this choice can have repercussions on the fracture parameters calculated, much care must been taken about choosing this limit.

An important result of this work is that the thickness has a high effect on the fracture values of this material. Thus, an increase of t has produced a clear drop in w_e, a result that can be justified by the fracture surfaces observed by SEM. Nevertheless, it must be taken in account that not all the variation can be attributed to the thickness change, since we detected variations in cristallinity depending on the preparation method. To explain the reasons of such a behavior, further work is being done.

The authors of this study wish to thank Tecniplàstica Extrusió for supplying the material, and Dr. I. Irribaren for the X-Ray scattering analysis. D. Ferrer is grateful for a doctoral grant from the CICYT.

REFERENCES

1. Mai, Y. W.; Cotterell, B. Int J of Fracture 1986, 32, 105.
2. Mai, Y. W.; Cotterell, B.; Horlyck R.; Vigna, G. Polym Eng Sci 1987, 27, 804.
3. Broberg, K. B. Int. J of Fracture 1968, 4, 11.
4. Saleemi, A. S.; Nairn, J. A. Polym Eng Sci 1990, 30, 211.
5. Hashemi, S. J Mater Sci 1993, 28, 6178.
6. Hashemi, S. J Mater Sci 1997, 32, 1563.
7. Hashemi, S. Polym Eng Sci 1997, 37, 912.
8. Chan, W. Y. F.; Williams, J. G. Polymer 1994, 35, 1666.
9. Wu, J.; Mai, Y. W. Polym Eng Sci 1996, 36, 2275.
10. Levita, G.; Parisi, L.; Marchetti, A. J Mater Sci 1994, 29, 4545.
11. Levita, G.; Parisi, L.; McLoughlin, S. J Mater Sci 1996, 31, 1545.
12. Levita, G.; Parisi, L.; Marchetti, A.; Bartolommei, L. Polym Eng Sci 1996, 36, 2534.
13. Maspoch, M. Ll.; Santana, O. O.; Grando, J.; Ferrer, D.; Martinez, A. B. Pol Bull 1997, 39, 249.
14. Karger-Kocsis, J. Pol Bull 1996, 37, 119.
15. Karger-Kocsis, J.; Czigány, T.; Moskala, E. Polymer 1997, 18, 4587.
16. Broek, D. Elementary engineering fracture mechanics, 3rd de.; Martinus Nijhoff, Leiden; 1982.
17. ESIS-TC4, Testing Protocol For Essential Work of Fracture 1993.
18. Hill, R. H. J Mech Phys Solids 1952, 4, 19.
19. Frontini, P. M.; Fave, A. J Mater Sci 1995, 30, 2446.